Luminescence properties of Eu^{3+} and Ti^{IV}/Zr^{IV} doped yttrium oxysulfides ($Y_2O_2S:Eu^{3+},Ti^{IV}/Zr^{IV}$)

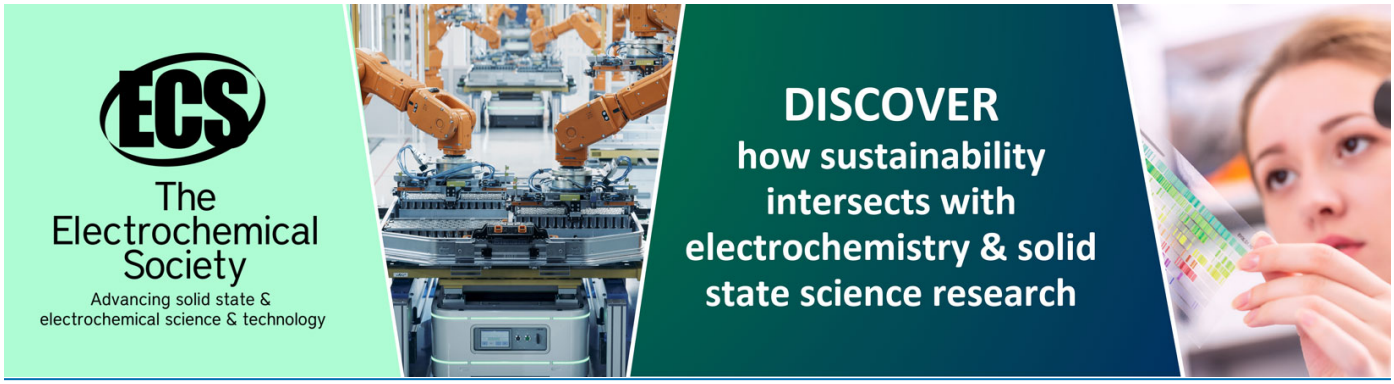

IOP Conf. Series: Materials Science and Engineering **15** (2010) 012085 doi:10.1088/1757-899X/15/1/012085

Luminescence properties of Eu^{3+} and Ti^{IV}/Zr^{IV} doped yttrium oxysulfides ($Y_2O_2S:Eu^{3+},Ti^{IV}/Zr^{IV}$)

H Bettentrup[1], KO Eskola[2], J Hölsä[3,4], A Kotlov[5], M Lastusaari[3,4] and M Malkamäki[3,6,*]

[1] Münster University of Applied Sciences, Stegerwaldstrasse 39, D-48565 Steinfurt, Germany
[2] University of Helsinki, Dating Laboratory, FI-00014 Helsinki, Finland
[3] University of Turku, Department of Chemistry, FI-20014 Turku, Finland
[4] Turku University Centre for Materials and Surfaces (MatSurf), Turku, Finland
[5] Deutsches Elektronen-Synchrotron, a Research Centre of the Helmholtz Association, Notkestrasse 85, D-22607 Hamburg, Germany
[6] Graduate School of Materials Research (GSMR), Turku, Finland

* Corresponding author: mhmalk@utu.fi

Abstract. The red emitting $Y_2O_2S:Eu^{3+},Ti^{IV}$ (or Zr^{IV}, x_{Eu}: 0.01, $x_{Ti/Zr}$: 0.003/0.015/0.03) materials were prepared with a flux method. According to X-ray powder diffraction, the materials have the hexagonal crystal structure. The UV excited (λ_{exc}: 250 nm) emission maximum was observed at 628 nm due to the $^5D_0 \rightarrow {}^7F_2$ transition of Eu^{3+}. The excitation spectra (λ_{em}: 628 nm) consist of broad bands centered at 240 and 320 nm due to the charge transfer transitions $O^{2-} \rightarrow Eu^{3+}$ and $S^{2-} \rightarrow Eu^{3+}$, respectively. Red persistent luminescence was observed with a maximum at 628 nm, as well. Persistent luminescence was the strongest with the Ti^{IV} co-doping though the intensity of persistent luminescence decreased with the increasing amount of both the Ti^{IV} and Zr^{IV} co-dopants. The thermoluminescence (TL) glow curves of the $Y_2O_2S:Eu^{3+},Ti^{IV}$ materials consist of bands at *ca.* 110 and 200 °C. In $Y_2O_2S:Eu^{3+},Zr^{IV}$, similar bands are observed at lower temperatures *viz.* at *ca.* 100 and 180 °C. TL weakens when the amount of co-dopants is increased. The Ti^{IV} co-doped materials have stronger TL than the Zr^{IV} co-doped materials. The deconvolution of TL glow curves revealed three distinct traps with depths ranging from 0.6 to 1.0 eV.

1. Introduction

Persistent luminescence materials continue to emit for several hours after the irradiation source has been removed. The best materials at present are the blue emitting disilicates (*e.g.* $Sr_2MgSi_2O_7:Eu^{2+},Dy^{3+}$ [1]) and blue/green emitting aluminates (*e.g.* $CaAl_2O_4:Eu^{2+},Nd^{3+}$ [2] and $SrAl_2O_4:Eu^{2+},Dy^{3+}$ [3]). Their persistent luminescence can be seen for up to 24 hours and they are (or may be) used in many applications such as traffic and emergency signs, watches, clocks and textile printing.

The development of stable and efficient red emitting persistent luminescence materials has turned out to be difficult even though they would be useful in many applications including medical diagnostics. One of the obstacles with these materials is that the sensitivity of the human eye is poor for the red light. Thus, the red emission should be very strong in order to compete with the green and

blue emitting materials. At the moment, known red emitting materials include *e.g.* the europium doped alkaline earth metal sulfides MS:Eu^{2+} [4] and oxides MO:Eu^{3+} [5,6] (M: Ca, Sr, Ba). These materials, however, are not chemically stable, and the duration of persistent luminescence is short, too. Another material is Y_2O_2S:Eu^{3+},Mg^{2+},Ti^{IV} which can emit for three hours after ceasing the irradiation [7-12].

The persistent luminescence of the yttrium oxysulfide materials has been explained to be due to defects created by the Mg^{2+} and Ti^{IV} doping. These defects can act as trap centers where the energy (electrons/holes) is stored. When the electrons/holes gain enough thermal energy they can leave the traps and persistent luminescence is observed. However, the mechanism of persistent luminescence and the effect of the co-dopants are not clear, and need further studies. Also the intensity and duration of the persistent luminescence of Y_2O_2S:Eu^{3+},Mg^{2+},Ti^{IV} should be enhanced to meet the requirements of applications.

When the Y_2O_2S:Eu^{3+} material is co-doped with Ti^{IV} the existence of Ti^{3+} cannot be ruled out because Ti^{IV} is easily reduced to Ti^{3+}. If Zr^{IV} is used instead of Ti^{IV}, the reduction of the co-dopant is not possible due to the high reduction potential of Zr^{IV}. Thus, only the charge compensation defects are present in the Zr^{IV} co-doped materials. Using the Kröger-Vink notation, two Ti^{IV}/Zr^{IV} ions in two Y^{3+} sites will create two defects with a positive net charge which can be compensated with an interstitial oxide ion (Equation 1). It is also possible that three Ti^{IV}/Zr^{IV} ions in three Y^{3+} sites will be compensated with an Y^{3+} vacancy (Equation 2).

$$2Y_Y^{\times} \rightarrow 2Ti_Y^{\bullet} + O_i^{''} \quad (1)$$

$$3Y_Y^{\times} \rightarrow 3Ti_Y^{\bullet} + V_Y^{'''} \quad (2)$$

In this work, the europium (Eu^{3+}) doped yttrium oxysulfides (Y_2O_2S:Eu^{3+}) co-doped with nominally tetravalent titanium (Ti^{IV}) or zirconium (Zr^{IV}) were prepared with a direct solid state reaction using a flux. The crystal purity and structure of the materials were studied with X-ray powder diffraction (XPD). The effect of the co-doping on the photo- and persistent luminescence was investigated by UV excitation, too. The band gap of the materials was estimated from the synchrotron radiation excitation spectra of Eu^{3+} measured at the SUPERLUMI station of HASYLAB at DESY (Hamburg, Germany). The thermoluminescence (TL) glow curves were measured and the depth of the traps was determined by the deconvolution of the TL curves.

2. Experimental

First, polycrystalline Y_2O_3:Eu^{3+},Ti^{IV}/Zr^{IV} materials were prepared by heating intimately mixed, stoichiometric amounts of Y_2O_3, Eu_2O_3 and TiO_2 (or $ZrO(NO_3)_2 \cdot 6H_2O$) at 1300 °C for five hours in air. The nominal amounts of Eu^{3+} and Ti^{IV}/Zr^{IV} were 1 and 0.3, 1.5 or 3 mole-% of the yttrium amount, respectively. After that, the Y_2O_2S:Eu^{3+},Ti^{IV}/Zr^{IV} materials were prepared with the flux method by adding Na_2CO_3 and S to the mixed oxide and heating the mixture at 900 °C for six hours in a static N_2 sphere. The mole ratio of Y_2O_3:Na_2CO_3:S was 1:1:3.4. The products were washed with dilute acetic acid and distilled water. The structural and phase purity was confirmed by X-ray powder diffraction using a Huber G670 image plate (2θ range: 4-100°) Guinier camera at 298 K ($CuK_{\alpha 1}$ radiation, 1.5406 Å). The measured patterns were compared to the calculated ones obtained with the program PowderCell [13] and structural data for Y_2O_2S [14].

The emission and excitation spectra of the materials were measured with a Varian Cary Eclipse spectrometer between 400-750 and 220-550 nm, respectively. The excitation source was a 15 W Xe lamp. Persistent luminescence spectra were measured 0.5 minutes after the irradiation with a 254 nm UV lamp (4 W) for five minutes. The intensity of persistent luminescence was obtained by integrating the peak at 628 nm. The synchrotron radiation excitation spectra were measured at 10 K with a 2 m Mc Pherson type monochromator at the SUPERLUMI station of HASYLAB at DESY (Hamburg, Germany).

The TL glow curves were measured with an upgraded Risø TL/OSL-DA-12 system using a constant heating rate of 5 °Cs^{-1} in the temperature range from 0 to 400 °C. The global TL emission from UV to 650 nm was monitored. Prior to the TL measurements, the samples were irradiated with a

combination of the Phillips TL 20W/05 (emission maximum at 360 nm) and TL 20W/03 (420 nm) UV lamps for 60 to 120 s. A delay time of 3 min between the irradiation and measurement was used. The analysis of the TL glow curves was carried out by deconvoluting the TL curves with the program TLanal v.1.0.3 [15,16] which uses the general approximation (GA) method as a background. The fitted peaks were considered to be of the 2nd order kinetics because of their symmetric shape.

3. Results and discussion

3.1. Crystal structure and purity

All oxysulfide materials crystallized (Figure 1) in the hexagonal structure (space group $P\bar{3}m1$, No. 164, Z: 1) with *a*: 3.750 and *c*: 6.525 Å [16]. The structure has only one eight coordinated Y^{3+} site with a C_{3v} point symmetry. Impurity compounds were not observed which means that the Ti^{IV} and Zr^{IV} co-dopants have entered the Y^{3+} sites. Thus, a solid solution is apparently formed although the ionic radii are different between Y^{3+} (1.019 Å) and Ti^{IV}/Zr^{IV} (0.74/0.84) [17]. The ionic radius of Ti^{3+} for the coordination number eight was not found in the literature. Instead, with the coordination number six, it is 0.670 Å. For Ti^{IV} the ionic radii for the coordination numbers six and eight are 0.605 and 0.74 Å, respectively. Assuming a constant difference of *ca.* 0.14 Å, the ionic radius of Ti^{3+} with coordination number eight is *ca.* 0.81 Å. This is much closer to the ionic radius of Y^{3+} which also supports the fact that Ti^{IV} can be reduced to Ti^{3+}.

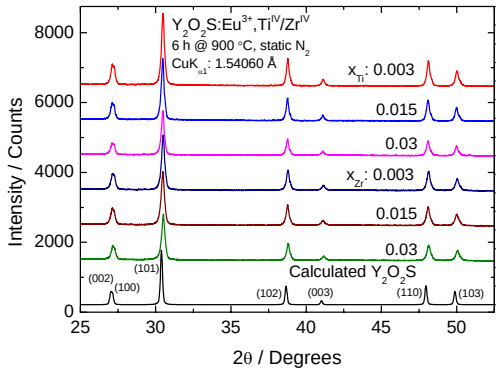

Figure 1. X-ray powder diffraction patterns of the $Y_2O_2S:Eu^{3+}$ materials with different amounts of the Ti^{IV} and Zr^{IV} co-dopants. The reference pattern was calculated with the PowderCell program [13] using the crystallographic data from [14].

3.2. Emission and excitation

The red emission of $Y_2O_2S:Eu^{3+},Ti^{IV}/Zr^{IV}$ has a maximum at 628 nm due to the $^5D_0 \rightarrow {}^7F_2$ transition of Eu^{3+} (Figure 2, left). Weaker emission lines above 450 nm are due to the other $^5D_{0,1,2} \rightarrow {}^7F_{0\text{-}4}$ transitions. The emission spectra are rather similar irrespective of the co-dopant amount. The photocatalysed $Ti^{IV} \leftrightarrow Ti^{3+}$ redox reactions seem to have no effect. The luminescence intensity of the Zr^{IV} co-doped materials is the highest with the lowest co-doping level (0.003) though the luminescence drastically weakens when the co-dopant amount increases. Also a slight weakening of emission with the increasing Ti^{IV} amount is observed but is less pronounced than with Zr^{IV}.

In the excitation spectra, two broad bands are observed at 250 and 330 nm (Figure 2, right). These bands are due to the $O^{2-}(2p) \rightarrow Eu^{3+}$ and $S^{2-}(3p) \rightarrow Eu^{3+}$ charge transfer (CT) transitions, respectively. In the Ti^{IV} co-doped materials, the band at 330 nm can also be due to the energy transfer from Ti^{IV} to Eu^{3+} which is a consequence of the charge transfer transition $O^{2-}(2p) \rightarrow Ti^{IV}(3d)$ [10,18]. The weak lines between 375 and 550 nm are due to the $^7F_{0,1} \rightarrow {}^5D_{1,2,3}$ transitions of Eu^{3+}.

The amount of Ti^{IV} co-dopants does not affect the CT band from O^{2-} significantly but the intensity of the CT band from S^{2-} is slightly decreasing with the increasing amount of the co-dopant. In the Zr^{IV} co-doped materials, the intensity of the O^{2-} CT band decreases significantly as the amount of the Zr^{IV} co-dopant increases. Also the S^{2-} CT band weakens but the effect is weaker. There are no significant changes in the intensities of the weak $^7F \rightarrow {}^5D$ lines. The loss of intensity with the increasing co-dopant amount may be due to the fact that the excitation energy is stored to traps. In the Zr^{IV} co-doped

materials the amount of defects is higher because only the charge compensation is possible. Thus the excitation energy is stored more efficiently and the UV excited luminescence is weakened.

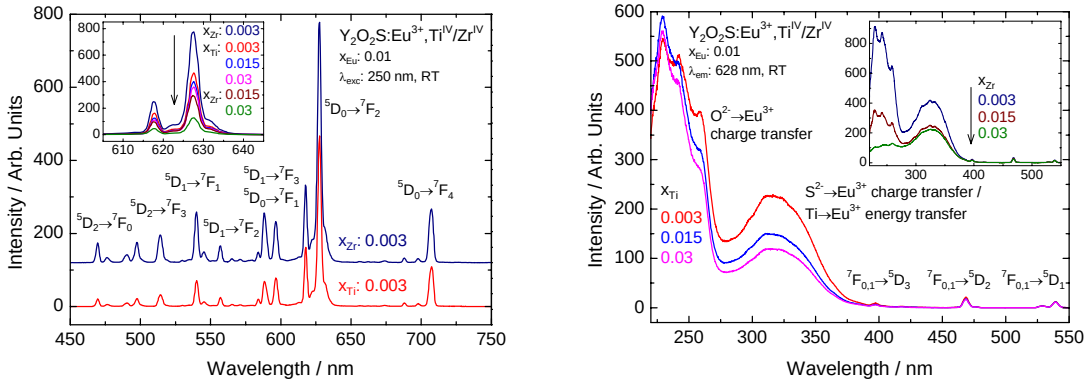

Figure 2. Emission (left) and excitation (right) spectra of $Y_2O_2S:Eu^{3+},Ti^{IV}/Zr^{IV}$.

In the synchrotron radiation excitation spectra (Figure 3) of $Y_2O_2S:Eu^{3+}$, the valence to conduction band absorption edge is observed at 260 nm which gives *ca.* 4.8 eV as the energy gap of Y_2O_2S. This is in a good agreement with the literature values 4.6-4.8 eV [19]. The $S^{2-}\rightarrow Eu^{3+}$ CT band can be observed at 320 nm which corresponds well to the conventional UV measurements. In the Ti^{IV} co-doped material, the structure of the spectrum is lost and the absorption edge is not so easily observed. However, a peak in the derivative curve at 260 nm is observed, indicating that the band gap does not change significantly with Ti^{IV} co-doping. In both spectra, no clear excitonic features are observed around the bottom of the conduction band.

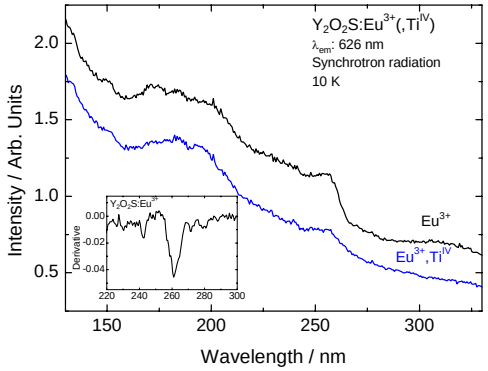

Figure 3. Synchrotron radiation excitation spectra of the $Y_2O_2S:Eu^{3+}(,Ti^{IV})$ materials. Insert: derivative of the excitation spectrum of $Y_2O_2S:Eu^{3+}$.

3.3. Persistent luminescence

Weak red persistent luminescence is observed in the $Y_2O_2S:Eu^{3+},Ti^{IV}/Zr^{IV}$ materials with UV irradiation. The maximum is observed at 628 nm which is the same as in the photoluminescence spectra (Figure 4, left). It is due to the $^5D_0\rightarrow{}^7F_2$ transition of Eu^{3+}. The details of the spectra are lost because wide emission slits were used in the measurements. However, the persistent luminescence emission spectra are different in the Ti^{IV} and Zr^{IV} co-doped materials. The spectrum of the Zr^{IV} co-doped $Y_2O_2S:Eu^{3+}$ comprises also the weak $^5D_{0,1,2}\rightarrow{}^7F_{0\text{-}4}$ transitions of Eu^{3+}. For the Ti^{IV} co-doped materials these transitions between 450 and 595 nm are not observed. Instead, there is a broad band between 525 and 725 nm in the spectrum. A similar band in the photo- and/or persistent luminescence spectra of the Ti^{3+} doped $R_2O_2S:Ti$ (R: Y, Gd) materials has been observed centered at *ca.* 590 nm [20-

24]. This band was attributed to the Ti doping and may be due to the $^2E \rightarrow {}^2T_2$ transition of Ti^{3+}, based on the similarity with the $CaGdAlO_4:Ti^{3+}$ emission at *ca.* 600 nm [25]. The differences in the persistent luminescence emission spectra between the Ti^{IV} and Zr^{IV} co-doped materials suggest that the excitation mechanisms are different. The Ti^{IV} co-doped material emits from only the $^5D_0$ level of Eu^{3+} whereas the Zr^{IV} co-doped material emits from the higher ^5D levels, too. This is due to the feeding of excitation energy from traps to the Ti^{3+} levels and then further to the $^5D_0$ level of Eu^{3+} thus going past the higher ^5D levels of Eu^{3+}.

The persistent luminescence of the $Y_2O_2S:Eu^{3+},Ti^{IV}/Zr^{IV}$ materials weakens with the increasing amount of the co-dopants (Figure 4, right). Also, the persistent luminescence of the Ti^{IV} co-doped materials is stronger than in the Zr^{IV} co-doped materials. The most intense persistent luminescence was observed in the Ti^{IV} co-doped material with 0.3 mole-% of the co-dopant. The differences in the persistent luminescence efficiency (intensity and duration) can be explained with the different trap structures to be described in detail in the next section.

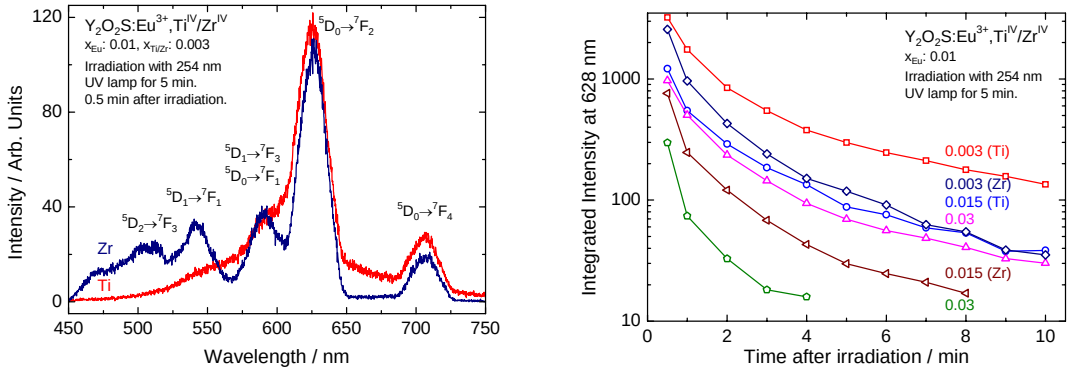

Figure 4. Persistent luminescence emission spectra (left) and persistent luminescence intensity after irradiation (right) of the $Y_2O_2S:Eu^{3+},Ti^{IV}/Zr^{IV}$ materials.

3.4. Thermoluminescence

The thermoluminescence (TL) glow curves of the Ti^{IV} co-doped $Y_2O_2S:Eu^{3+}$ materials consist of two main peaks corresponding to shallow and deep traps at *ca.* 110 and 200 °C, respectively (Figure 5). In the Zr^{IV} co-doped materials, similar two peaks appear at lower temperatures *viz.* at 100 and 180 °C. The TL intensity of the Zr^{IV} co-doped materials is significantly weaker than that of the Ti^{IV} co-doped materials though the $^5D_{1,2}$ emissions partly compensate for this difference. This means that the trap density is lower in the Zr^{IV} co-doped $Y_2O_2S:Eu^{3+}$ and thus the ability to store energy is weaker. In both the Ti^{IV} and Zr^{IV} co-doped materials, the TL intensity weakens with increasing co-dopant amount. This is due to the change in the trap structure which leads to different energy storage properties.

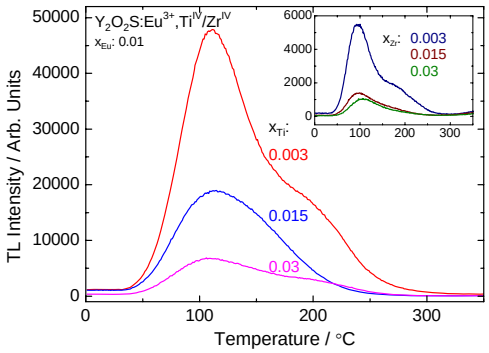

Figure 5. TL glow curves of the $Y_2O_2S:Eu^{3+},Ti^{IV}/Zr^{IV}$ materials.

The deconvolution of the TL curves reveals three traps (Figure 6, left). The traps possess depths between 0.6 and 1.0 eV and the TL peaks follow the 2nd order kinetics. However, the trap structures obtained are rather similar, perhaps with the exception of the Zr^{IV} (0.015) material (Figure 6, right). The change in the trap structure with the increasing co-dopant amounts and the corresponding

decrease in both the thermo- and persistent luminescence can thus be explained only by the creation of shallower traps – not observed in the TL measurements above the room temperature. The strong initial decrease in the persistent luminescence intensity *i.e.* the immediate emptying of the shallow traps (Figure 4, right), supports this reasoning. This effect may be due also to the narrower spread of the trap depth distributions in the Zr doped materials allowing for an immediate emptying of the traps after ceasing the irradiation. Low temperature TL measurements are evidently needed to clarify this hypothesis.

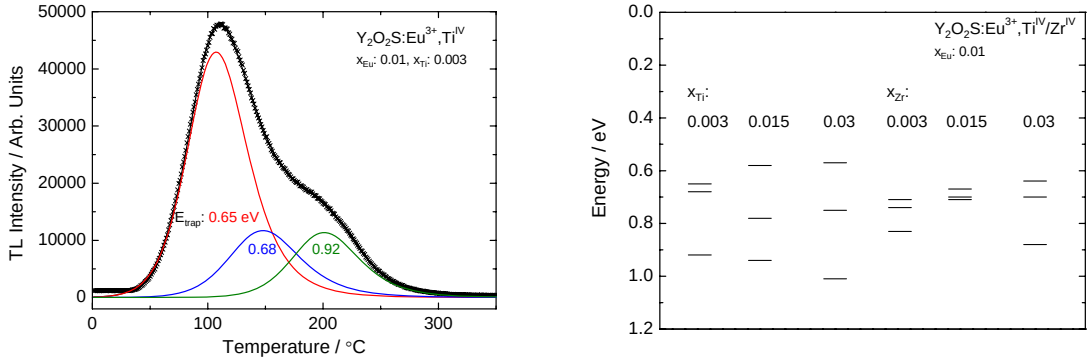

Figure 6. Deconvoluted TL glow curve of $Y_2O_2S:Eu^{3+},Ti^{IV}$ with x_{Ti}: 0.003 (left) and trap depths obtained by deconvolution of TL glow curves (right) of the $Y_2O_2S:Eu^{3+},Ti^{IV}/Zr^{IV}$ materials.

4. Conclusions

Red persistent luminescence with a maximum at 628 nm was observed in both the Ti^{IV} and Zr^{IV} co-doped $Y_2O_2S:Eu^{3+}$ materials. The persistent luminescence in the Ti^{IV} co-doped materials is stronger than in the Zr^{IV} co-doped materials. The TL measurements reveal the better ability of the Ti^{IV} co-doped materials to store energy, especially for longer times. The strongest persistent luminescence was observed with the lowest Ti^{IV}/Zr^{IV} co-doped amounts. An increase in the concentration of charge compensation defects further seems to be counterproductive. On the other hand, persistent luminescence is not observed at all without co-doping. There are differences in the persistent luminescence emission spectra between the Ti^{IV} and Zr^{IV} co-doped materials, which means that they have different excitation mechanisms. In the future, the study of the delicate interplay between different energy level systems (host band gap, Eu^{3+} and Ti^{3+} as well as trap levels) will clarify the persistent luminescence mechanism which, as a whole, is completely undisclosed for Eu^{3+} systems.

Acknowledgements

Financial support from the Academy of Finland (project #8117057/2007) to M.M. is acknowledged. Parts of this research were carried out at the light source facility Doris III at HASYLAB/DESY. DESY is a member of the Helmholtz Association (HGF). The research leading to these results has received funding from the European Community's Seventh Framework Programme (FP7/2007-2013) under grant agreement No. 226716.

References

[1] Lin Y, Nan CW, Zhou X, Wu J, Wang H, Chen D and Xu S, 2003 *Mater. Chem. Phys.* **82** 860-3.
[2] Yamamoto H and Matsuzawa T, 1997 *J. Lumin.* **72-74** 287-9.
[3] Matsuzawa T, Aoki Y, Takeuchi N and Murayama Y, 1996 *J. Electrochem. Soc.* **143** 2670-3.
[4] Jia D and Wang X, 2007 *Opt. Mater.* **30** 375-9.

[5] Fu J, 2000 *Electrochem. Solid-State Lett.* **3** 350-1.
[6] Fu J, 2002 *J. Am. Ceram. Soc.* **85** 255-7.
[7] Wang X, Zhang Z, Tang Z and Lin Y, 2003 *Mater. Chem. Phys.* **80** 1-5.
[8] Zhang J, Zhang Z, Tang Z and Wang T, 2004 *Ceram. Int.* **30** 225-8.
[9] Wang Y and Wang Z, 2006 *J. Rare Earths* **24** 25-8.
[10] Hölsä J, Laamanen T, Lastusaari M, Malkamäki M, Niittykoski J and Zych E, 2009 *Opt. Mater.* **31** 1791-3.
[11] Li W, Liu Y, Ai P and Chen X, 2009 *J. Rare Earths* **27** 895-9.
[12] Li W, Liu Y and Ai P, 2010 *Mater. Chem. Phys.* **119** 52-6.
[13] Kraus W and Nolze G, Powder Cell for Windows, version 2.4, Federal Institute for Materials Research and Testing, Berlin, Germany, 2000.
[14] Mikami M and Nakamura S, 2006 *J. Alloys Compd.* **408-412** 687-92.
[15] Chung KS, TL Glow Curve Analyzer v.1.0.3., Korea Atomic Energy Research Institute and Gyeongsang National University in Korea, 2008.
[16] Chung KS, Choe HS, Lee JI, Kim JL and Chang SY, 2005 *Rad. Prot. Dosim.* **115**, 345-9.
[17] Shannon RD, 1976 *Acta Cryst. A* **32** 751-67.
[18] Bettentrup H, Hölsä J, Laamanen T, Lastusaari M, Malkamäki M, Niittykoski J and Zych E, 2009 *J. Lumin.* **129** 1661-3.
[19] Li S and Ahuja R, 2005 *J. Appl. Phys.* **97** 103711.
[20] Kang CC, Liu RS, Chang JC and Lee BJ, 2003 *Chem. Mater.* **15** 3966-8.
[21] Zhang P, Hong Z, Wang M, Fang X, Qian G and Wang Z, 2005 *J. Lumin.* **113** 89-93.
[22] Zhang P, Hong Z, Shen H, Xu Z and Fan X, 2006 *J. Rare Earths* **24** 115-8.
[23] Wang L, Zhang L, Huang Y, Jia D and Lu J, 2009 *J. Lumin.* **129** 1032-5.
[24] Lei B, Liu Y, Zhang J, Meng J, Man S and Tan S, 2010 *J. Alloys Compd.* **495** 247-53.
[25] Kodama N and Yamaga M, 1998 *Phys. Rev. B* **57** 811-7.